

CrystEngComm

Accepted Manuscript



This is an *Accepted Manuscript*, which has been through the Royal Society of Chemistry peer review process and has been accepted for publication.

Accepted Manuscripts are published online shortly after acceptance, before technical editing, formatting and proof reading. Using this free service, authors can make their results available to the community, in citable form, before we publish the edited article. We will replace this *Accepted Manuscript* with the edited and formatted *Advance Article* as soon as it is available.

You can find more information about *Accepted Manuscripts* in the [Information for Authors](#).

Please note that technical editing may introduce minor changes to the text and/or graphics, which may alter content. The journal's standard [Terms & Conditions](#) and the [Ethical guidelines](#) still apply. In no event shall the Royal Society of Chemistry be held responsible for any errors or omissions in this *Accepted Manuscript* or any consequences arising from the use of any information it contains.

EBSD-Measurements of Textured Apatite Glass-Ceramics

Wolfgang Wisniewski^{1*}, René de Kloe² and Christian Rüssel¹

¹Otto-Schott-Institut, Jena University, Fraunhoferstr. 6, 07743 Jena, Germany

²EDAX, Ringbaan Noord 103, Tilburg, The Netherlands

Summary

A silicate-phosphate-glass was placed into a furnace preheated to 1200 °C in order to crystallize rod-shaped fluoroapatite crystals. The partially crystalline melt is extruded to align the crystal rods, leading to oriented glass-ceramics with anisotropic mechanical properties. These glass-ceramics are cut parallel and perpendicular to the extrusion direction and treated using chemical etching, ion milling and polishing procedures in order to enable electron backscatter diffraction (EBSD) measurements. The ability to obtain EBSD-patterns is strongly affected by the crystal orientation and the glass-ceramics are shown to be sensitive towards the electron beam and hence susceptible to sample modification during EBSD-analyses.

*Corresponding author: Wolfgang Wisniewski

Fraunhoferstr. 6, 07743 Jena

Otto-Schott-Institut, Jena University

Tel: (0049) 03641 948515

Fax: (0049) 03641 948502

wolfgang.w@uni-jena.de

EBSD-Measurements of Textured Apatite Glass-Ceramics

Wolfgang Wisniewski^{1*}, René de Kloe² and Christian Rüssel¹

¹Otto-Schott-Institut, Jena University, Fraunhoferstr. 6, 07743 Jena, Germany

²EDAX, Ringbaan Noord 103, Tilburg, The Netherlands

Summary

A silicate-phosphate-glass was placed into a furnace preheated to 1200 °C in order to crystallize rod-shaped fluoroapatite crystals. The partially crystalline melt is extruded to align the crystal rods, leading to oriented glass-ceramics with anisotropic mechanical properties. These glass-ceramics are cut parallel and perpendicular to the extrusion direction and treated using chemical etching, ion milling and polishing procedures in order to enable electron backscatter diffraction (EBSD) measurements. The ability to obtain EBSD-patterns is strongly affected by the crystal orientation and the glass-ceramics are shown to be sensitive towards the electron beam and hence susceptible to sample modification during EBSD-analyses.

1. Introduction

Glasses and glass-ceramics used as implants for permanent or temporary bone replacements usually either form apatite on the surface in contact with the biological environment or already contain apatite.¹⁻⁴ These materials may then directly bond to the human bone without the formation of an interconnecting tissue.

Glasses allowing the crystallization of apatite have been described in the literature.^{5,6} One drawback of these materials is their fairly low mechanical strength of usually below 100 MPa. Apatite containing glass-ceramics with aligned, rod-shaped apatite crystals have been prepared by the extrusion of a partially crystalline melt.⁷⁻¹³ While the apatite orientation does not lead to an anisotropic hardness of the glass-ceramic, anisotropic crack propagation was detected.⁷ A mechanical toughness of up to $1.46 \text{ MPa}\cdot\text{m}^{-1/2}$ has been reported perpendicular to the extrusion direction while it was only $0.9 \text{ MPa}\cdot\text{m}^{-1/2}$ parallel to the extrusion direction.⁷

In the past, a crystallographic texture with the c-axes preferably oriented parallel to the extrusion direction while the a- and b-axes orientations are randomly distributed has been described using X-ray diffraction (XRD),⁷⁻¹¹ and texture goniometry.⁹ The texture is especially relevant because the orientation of the apatite crystals inside a biomaterial widely affects the growth of dentine and supposedly also that of bone in a biological environment.^{14,15} This has been shown for the growth of dentine on oriented apatite glass-ceramics in mineralizing solutions with the support of a leucin-rich amelogenin peptide. The apatite crystals of the dentin grow preferentially in the direction of the crystallographic c-axis of the apatite.

This paper features glasses in the system $\text{SiO}_2/\text{Al}_2\text{O}_3/\text{CaO}/\text{P}_2\text{O}_5/\text{Na}_2\text{O}/\text{K}_2\text{O}/\text{F}^-$. If these glasses are heated slowly, a liquid/liquid phase separation occurs which leads to the formation of droplets

enriched in F, P and Ca while depleted of Al and Si.¹² Secondary droplets inside the primary droplets have also been described which contain elevated Al concentrations and may crystallize to form AlPO_4 .¹² The primary droplets crystallized to apatite which then has an approximately spherical shape. If, however, these glasses are rapidly heated by transferring them to a furnace preheated to 1200 °C, the phase separation is prevented and rod-shaped apatite crystals are formed. The aspect ratio of these rods is limited due to intracrystalline Ostwald ripening¹³; the details of the time dependent crystal development at various temperatures have been described elsewhere.^{6,11,13}

During the extrusion of a melt containing these anisotropic crystals, the formation of oriented structures is closely related to the occurrence of shear thinning, i.e. non-Newtonian flow behavior above a certain shear stress.^{10,11} Below the threshold where Newtonian behavior is observed, the alignment of anisotropic flow units does not take place.^{10,11} Above the threshold, the morphology of the apatite crystals has a large effect on the flow behavior of the melt.¹⁰

Extrusion has also been used to produce oriented glass-ceramics containing mica,¹⁶⁻¹⁸ where a glass containing plate-like crystals was extruded. In the case of lithium disilicate glass-ceramics, orientation is also achieved by extruding the uncrystallized glass and subsequently annealing it.^{18,19} By contrast, extruding the glass used for the apatite formation before the crystallization did not result in a subsequent oriented crystal growth in this system.⁹

Recent studies of oriented glass-ceramics using electron backscatter diffraction (EBSD) in a scanning electron microscope (SEM) have shown that this method frequently provides novel insights into crystal orientations and textures in these systems. EBSD enables to obtain local

orientation information down to the nm scale allowing a much more detailed insight into crystal orientations compared to the texture measurement methods noted above.

Up to now, this method has typically been used to determine the texture in glass-ceramics crystallized using localized nucleation, such as surface crystallization²¹⁻²⁵ or electrochemically induced crystallization.^{26,27} Here EBSD has shown that surface crystallization is frequently initiated by oriented nucleation^{21,24} while the textures observed after electrochemically induced nucleation are rather a result of the experimental setup instead of oriented nucleation or growth along an electrical field.^{26,27}

In this article we apply EBSD to oriented apatite glass ceramics produced by the extrusion of a partially crystalline melt. It is the first report featuring EBSD-analyses of extruded glass-ceramics.

2. Results and Discussion

Figure 1 shows XRD-patterns of samples cut a) parallel and b) perpendicular to the extrusion direction. All occurring peaks may be attributed to hexagonal fluoroapatite of the composition $\text{Ca}_2(\text{PO}_4)_3\text{F}$, but the intensities of the XRD-lines depend notably on the cut plane. In agreement with the literature,⁷⁻¹¹ the peaks attributed to the 002 and 004 planes are absent in pattern a) while they are of exaggerated intensity in pattern b) indicating a preferred orientation to the crystals with their c-axes aligned to the extrusion direction.

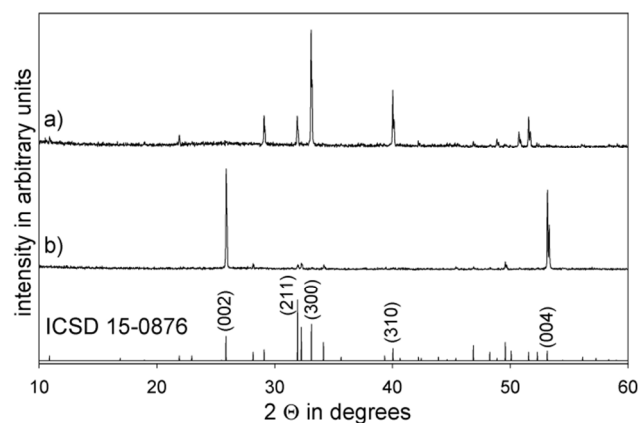


Figure 1: XRD-patterns of extruded glass ceramics cut: a) parallel and b) perpendicular to the extrusion direction. The pattern of JCPDS file 15-0876 representing apatite is shown for comparison.

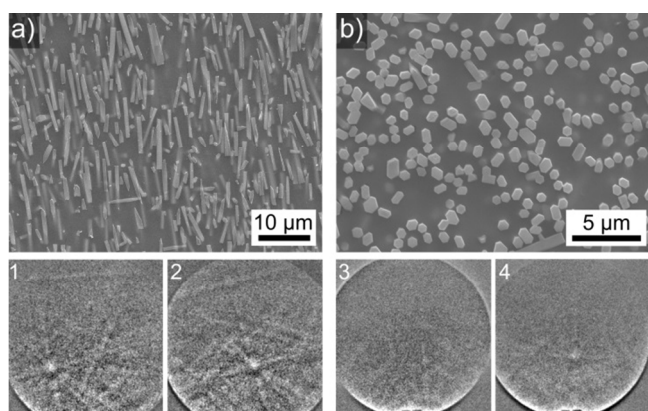


Figure 2: SEM-micrographs of cut planes a) parallel and b) perpendicular to the extrusion direction. While the EBSD-patterns 1 and 2 are representative of the cut plane a), the patterns 3 and 4 feature the best patterns obtainable from the sample and originate from elongated crystals which are probably not aligned to the extrusion direction.

Polished cut planes of extruded glass-ceramics cut a) parallel or b) perpendicular to the extrusion direction are presented in Figure 2 along with the EBSD-patterns 1-4 obtained from these surfaces. Please note that the pattern quality of crystals cut parallel to their long axes greatly exceeds that of crystals cut perpendicular to it. In fact the crystals forming very regular hexagons fail to provide any discernible EBSD-patterns independent of whether the final step of sample preparation was chemo-mechanical polishing, chemical etching or ion milling. The apatite crystals assume the morphology of rods with a hexagonal cross section as visualized by the etched surface presented in Figure 3 a). Applying ion beam milling to this surface led to the surface presented in Figure 3 b) without significantly increasing the ability to obtain EBSD-patterns.

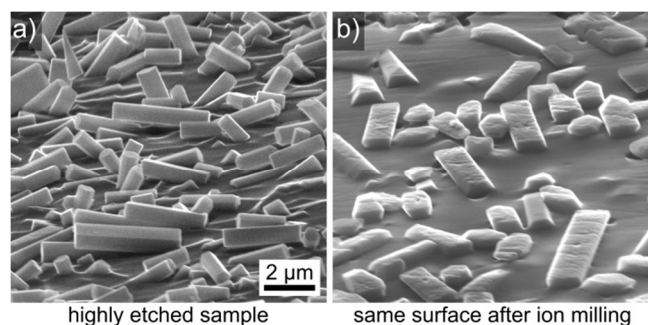


Figure 3: SEM-micrograph of a) an over etched surface tilted by 70° to offer a 3D impression of the apatite crystals in the glass-ceramic and b) the same sample after ion milling.

Figure 4 features a) an SEM-micrograph obtained using a voltage of 20 kV where the origins of the EBSD-patterns 1-8 are marked by the positions 1-8, b) an SEM-micrograph obtained using a voltage of 2 kV where surface modifications due to EBSD-pattern acquisition are highlighted by white arrows (patterns 1, 3 and 4), and c) a forward-scattering-detector (FSD) image obtained 7

from the surface. The FSD image is very sensitive to a strong orientation contrast and in this case shows that there is very little difference between the backscattering properties of crystals oriented perpendicular to each other. The clear difference in the pattern quality of the patterns 1-8 is independent from the polishing procedure or the carbon coating as the entire surface was treated homogeneously. Hence the difficulty to acquire EBSPs is mostly orientation dependent, either due to an orientation dependent sensitivity to the surface treatment or due to orientation dependent diffraction properties. Orientation dependent backscattering properties can be neglected based on the FSD-micrograph. While the patterns 1 and 2 (long axis of the crystal parallel to the surface) may be indexed reliably using a material file based on a fluoroapatite of hexagonal symmetry ((C6h)[6/m], $a=9.343 \text{ \AA}$, $c=6.823 \text{ \AA}$), the patterns 3-8 could not be indexed reliably.

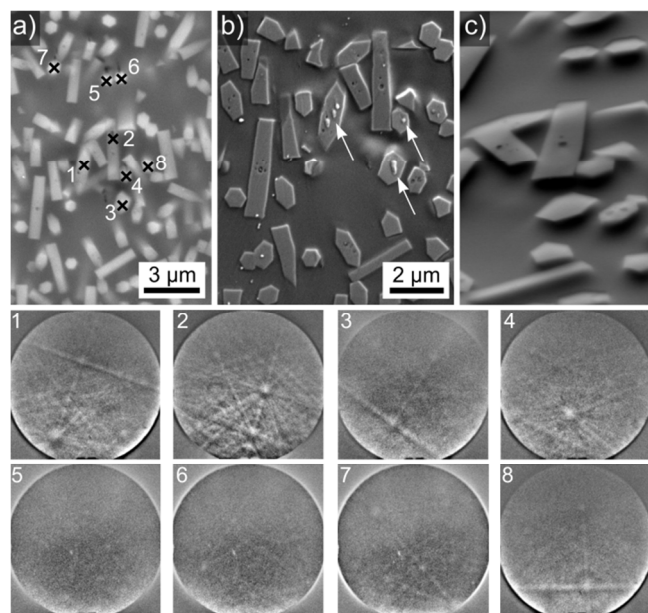


Figure 4: SEM-micrographs of a glass-ceramic with a lower degree of orientation obtained using the stated parameters. The EBSD-patterns 1-8 were acquired at the locations 1-8. The arrows highlight sample modifications caused by the EBSD-pattern acquisition. The FSD-micrograph shows no significant difference between the crystals independent of their cut plane.

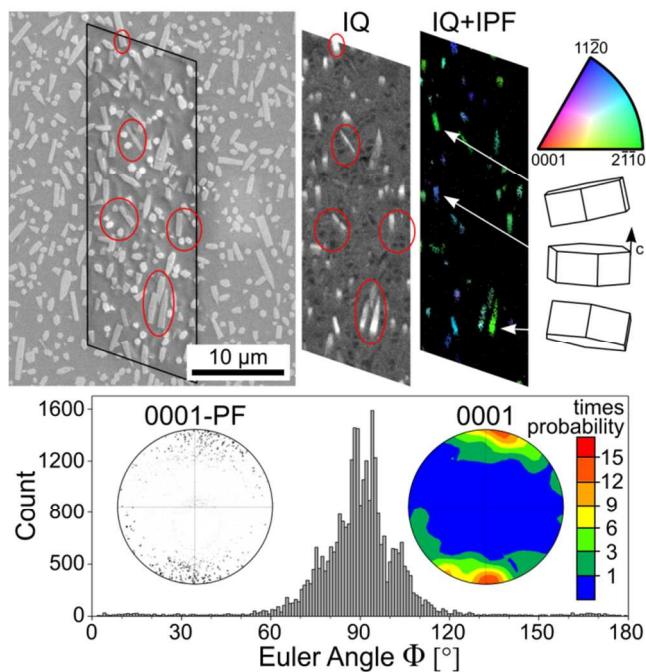


Figure 5: SEM-micrograph (2 kV) of a cut plane parallel to the extrusion direction superimposed by a frame indicating where an EBSD-scan was performed. The IQ-map of the entire scan as well as the IQ+IPF-map of a data set containing only points $CI > 0.1$ are presented as well as wire frames illustrating selected crystal orientations. The distribution of the Euler Angle Φ in a larger scan covering $43 \times 92 \mu\text{m}^2$ is presented below as well as the 0001-pole figure and 0001-texture of the data set.

An EBSD-scan was performed on the area framed in the SEM-micrograph of Figure 5. The image quality (IQ) map of the unfiltered dataset is presented and areas of interest are circled in red. Please note that the elongated crystals appear bright, indicating a relatively high IQ, while the locations of crystals cut perpendicular to their long axis actually appear darker than the glass matrix. These low IQ-values indicate that the EBSD patterns exhibit very low contrast where no bands are detected. If the same experiment is performed using no pattern processing or only the

background subtraction, these crystals receive slightly higher IQ-values than the residual glass due to their higher density. This effect has just recently been utilized in more detail while using the EBSD-camera for electron imaging.²⁸ The IPF+IQ-map of the CI-filtered data set hence only contains information on crystals which are oriented with their c-axis somewhat parallel to the surface as the wire frames of selected crystals illustrate. The distribution of the Euler Angle Φ , the 0001-pole figure (PF) and a 0001-texture calculated from a much larger scan covering an area of $43 \times 92 \mu\text{m}^2$ with a step size of 120 nm are presented below. The angle Φ describes the tilt of the c-axis of a crystal from the SEM-stage in this system; $\Phi=90^\circ$ indicates a c-axis parallel to the surface. The histogram implies that crystals with a c-axis tilted by more than ca. 30° from the polished cut plane do not provide reliably indexable EBSD-patterns. While the PF and texture show that the c-axes of the crystals are roughly aligned to the extrusion direction, these plots are not representative because many crystals showing orientations not matching the described texture do not produce EBSPs and hence do not occur in the datasets this analysis is based upon.

Figure 6 a) features a cut plane perpendicular to the extrusion direction after a performed EBSD-scan. The framed area is presented in greater detail in Figure 6 b) where traces of the electron beam can be discerned in the crystals as well as the matrix of the scanned part (right). The IQ-map of this part of the performed scan is presented in Figure 6 c): while the crystal cut parallel to its long axis shows high IQ-values and provided reliably indexable EBSD-patterns, the other crystals only show IQ-values slightly higher than the glass matrix and their orientation cannot be evaluated.

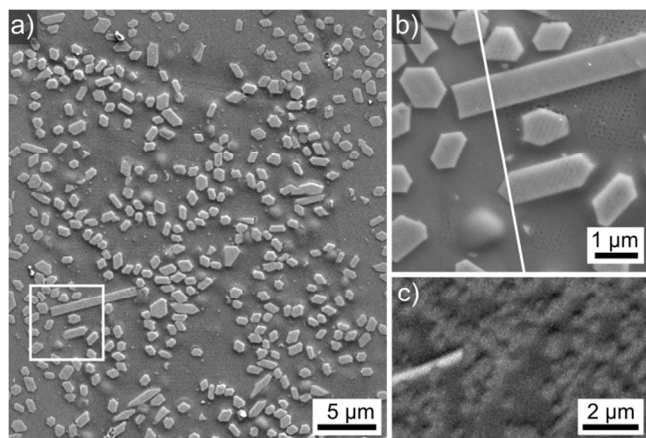


Figure 6: An extruded glass ceramic cut perpendicular to the extrusion direction after a performed EBSD-scan: a) SEM-micrograph, b) the framed area in higher detail: scan traces are clearly discernible in the right part. c) IQ-map of the apatite crystal cut parallel to its long axis and surrounded by apatite crystals cut perpendicular to their long axis as well as residual glass.

If the energy input per volume during an EBSD-scan is increased by e.g. decreasing the step size or applying a 2x2 binning instead of the 4x4 binning applied during the scans presented above, these glass ceramics are very sensitive to EBSD-pattern degradation which has been proposed to be mainly caused by the thermal buildup in the sample²⁹ as these materials have low thermal conductivities. Figure 7 presents SEM-micrographs obtained after EBSD-scans had been performed with a too high energy input for the glass-ceramic.

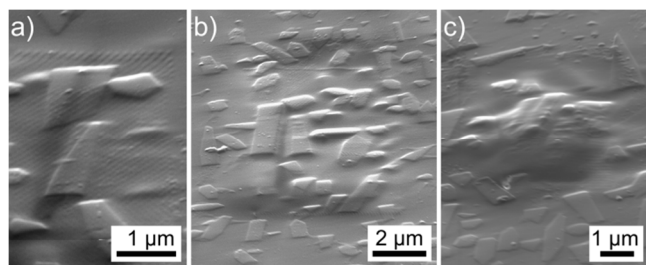


Figure 7: SEM-micrographs acquired after EBSD-scans performed with a to high energy input for the material: a) scan traces, b) slight swelling of the glass matrix and c) strong surface deformation.

3. Experimental

A silicate phosphate glass was prepared in batches of 75 g from SiO_2 (quartz), Na_2CO_3 , K_2CO_3 , CaCO_3 , $\text{Al}(\text{PO}_3)_3$, Na_3AlF_6 , K_3AlF_6 and $\text{AlOOH}\cdot\text{H}_2\text{O}$. The raw materials were melted in an alumina crucible at 1500 °C for 1 h and the resulting glass was cast into a carbon mold. It was then re-melted in a platinum crucible at 1550 °C for 1 h and again cast into a carbon mold. The cooled glass was cut into samples which were placed into a furnace preheated to 1200 °C where they were held for 1 h. The high heating rate prevented the liquid/liquid phase separation and hence resulted in the crystallization of rod-shaped fluoroapatite. The hot, partially crystalline melt was extruded from a Nicrofer chamber of an inner diameter of 21.5 mm using a Nicrofer piston. Extrusion was performed through a graphite die of 5 mm diameter using a velocity of 1 mm/min at temperatures in the range from 675 to 800 °C.

X-ray diffraction (XRD) was performed using $\text{CuK}\alpha$ -radiation in a SIEMENS *D5000* diffractometer.

In order to perform Scanning Electron Microscope (SEM) studies, crystallized and extruded samples were cut and polished with abrasive slurries down to diamond paste of 1 μm grain size. A final finish of 30 min using colloidal silica was applied. Some polished samples were etched using a 2% solution of HF/HNO₃ (1:1) for 20-40 s. Ion beam milling was performed using Ar ions in a BAL-TEC RES 010 mill and an incidence angle of ca. 5°. All samples were contacted with Ag-paste and coated with a thin layer of carbon at about 10⁻³ Pa to avoid surface charging in the SEM.

SEM analyses were performed using a scanning electron microscope (SEM Jeol *JSM 7001F*) equipped with an EDAX Trident analyzing system containing a Digiview 3 EBSD-camera. EBSD-scans were performed using a voltage of 20 kV and a current of ca. 2.40 nA. The scans were captured and evaluated using the software TSL OIM Data Collection 5.31 and TSL OIM Analysis 6.2. Unreliable data points were removed in all datasets used for orientation analysis by applying a Confidence Index (CI) filter of 0.1 after performing a grain CI standardization. This results in only considering orientation solutions which are correct with a probability of at least 95 % in EBSD-maps. No further cleanups which actually modify orientations were applied.

4. Conclusion

EBSA-analyses of the apatite crystals in these extruded glass-ceramics is possible. However, a highly orientation dependent ability to obtain EBSD-patterns after all the applied preparation techniques severely limits texture analysis. Patterns of sufficient quality for orientation analysis could only be obtained from crystals oriented with their c-axes more or less parallel to the cut plane with a maximum deviation of roughly $\pm 30^\circ$. This is especially noteworthy as the effect may

go unnoticed during the analysis of a sample containing randomly oriented apatite crystals but would then lead to the false description of a texture.

However, the partial results obtained using EBSD are in agreement with the results obtained by X-ray based methods. The apatite containing glass-ceramics featured in this article are quite sensitive to the electron beam and hence susceptible to sample modification during EBSD-analyses.

5. Acknowledgments

This work was supported by Deutsche Forschungsgemeinschaft (DFG) in Bonn Bad Godesberg (Germany) via project nr. RU 417/14-1.

References

1. T. Kokubo, H.-M. Kim, M. Kawashita, *Biomaterials* 2003, **24**, 2161–2175.
2. A. J. Salinas, M. Vallet-Regí, *RSC Adv.* 2013, **3**, 11116–11131.
3. G. Kaur, O. P. Pandey, K. Singh, D. Homa, B. Scott, G. Pickrell, *J. Biomed. Mater. Res. A* 2014, **102A**, 254-274.
4. O. Peitl, E. D. Zanotto, L. L. Hench, *J. Non-Cryst. Solids* 2001, **292**, 115-126.
5. C. Moiescu, C. Jana, C. Rüssel, *J. Non-Cryst. Solids* 1999, **248**, 169-175.
6. C. Moiescu, T. Höche, G. Carl, R. Keding, C. Rüssel, W. D. Heerdegen, *J. Non-Cryst. Solids* 2001, **289**, 123-134.
7. C. Moiescu, C. Jana, G. Carl, S. Habelitz, C. Rüssel, *Glastech. Ber. Glass Sci. Technol.* 1998, **71C**, 150-155.
8. C. Moiescu, C. Jana, C. Rüssel, S. Habelitz, G. Carl, *Adv. Sci. Technol.* 1999, **28**, 41-50.
9. C. Moiescu, C. Jana, S. Habelitz, G. Carl, C. Rüssel, *J. Non-Cryst. Solids* 1999, **248**, 176-182.
10. Y. Yue, C. Moiescu, G. Carl, C. Rüssel, *Phys. Chem. Glasses* 1999, **40**, 243-247.
11. C. Moiescu, G. Carl, C. Rüssel, *Glastech. Ber. Glass Sci. Technol.* 2000, **73**, 187-192.
12. T. Höche, C. Moiescu, J. Avramov, C. Rüssel, W. D. Heerdegen, *Chem. Mater.* 2001, **13**, 1312-1319.
13. T. Höche, C. Moiescu, J. Avramov, C. Rüssel, *Chem. Mater.* 2001, **13**, 1320-1325.
14. S. Habelitz, P. K. DenBesten, J. S. Marshall, G. W. Marshall, W. Li, *Eur. J. Oral Sci.* 2006, **111**, 315-319.
15. S. Habelitz, A. Kullar, J. S. Marshall, P. K. DenBesten, M. Balooch, G. W. Marshall, W. Li, *J. Dent. Res.* 2004, **83**, 698-702.
16. K. H. G. Ashbee, *J. Mater. Sci.* 1975, **10**, 911-917.
17. S. Habelitz, G. Carl, C. Rüssel, K. Marchetti, E. Roeder, D. Eifler, *Glastech. Ber. Glass. Sci. Technol.* 1997, **70**, 86-92.
18. S. Habelitz, G. Carl, C. Rüssel, S. Thiel, U. Gerth, J.-D. Schnapp, A. Jordanov, H. Knake, *J. Non-Cryst. Solids* 1997, **220**, 291-298.
19. D. I. H. Atkinson, P. W. McMillan, *J. Mater. Sci.* 1977, **12**, 443-450.
20. B. Durschang, G. Carl, C. Rüssel, K. Marchetti, E. Roeder, *Glastech. Ber. Glass Sci. Technol.* 1994, **67**, 171-177.
21. W. Wisniewski, K. Otto, C. Rüssel, *Cryst. Growth Des.* 2012, **12**, 5035-5041.
22. W. Wisniewski, S. Berndt, M. Müller, C. Rüssel, *CrystEngComm* 2013, **15**, 2392-2400.
23. A. Keshavarzi, W. Wisniewski, René de Kloe, C. Rüssel, *CrystEngComm* 2013, **15**, 5425-5433.
24. W. Wisniewski, C. Bocker, M. Kouli, M. Nagel, C. Rüssel, *Cryst. Growth Des.* 2013, **13**, 3794-3800.
25. W. Wisniewski, M. Patschger, C. Rüssel, *Sci. Rep. UK* 2013, **3**, 3558.
26. W. Wisniewski, M. Nagel, G. Völksch, C. Rüssel, *Cryst. Growth Des.* 2010, **10**, 1939-1945.
27. W. Wisniewski, R. Carl, G. Völksch, C. Rüssel, *Cryst. Growth Des.* 2011, **11**, 784-790.
28. S. I. Wright, M. M. Nowell, R. de Kloe, P. Camus, T. Rampton, *Ultramicroscopy* 2015, **148**, 132–145.

29. W. Wisniewski, G. Völksch, C. Rüssel, *Ultramicroscopy* 2011, **111**, 1712-1719.

Table of Contents Entry

EBSD-Measurements of Textured Apatite Glass-Ceramics

Wolfgang Wisniewski^{1*}, René de Kloe² and Christian Rüssel¹

¹Otto-Schott-Institut, Jena University, Fraunhoferstr. 6, 07743 Jena, Germany

²EDAX, Ringbaan Noord 103, Tilburg, The Netherlands

A partially crystallized glass melt is extruded to align the apatite crystals. An orientation dependent EBSD-pattern acquisition is observed, making texture analysis problematic.

